Renormalization group for link percolation on planar hyperbolic manifolds

Ivan Kryven

Mathematical Institute, Utrecht University, PO Box 80010, 3508 TA Utrecht, the Netherlands

Robert M. Ziff

Center for the Study of Complex Systems and Department of Chemical Engineering,
University of Michigan, Ann Arbor, Michigan 48109-2136, USA

Ginestra Bianconi

School of Mathematical Sciences, Queen Mary University of London, London, E1 4NS, United Kingdom
and Alan Turing Institute, 96 Euston Rd, London, NW1 2DB, United Kingdom

Network geometry is currently a topic of growing scientific interest, as it opens the possibility to explore and interpret the interplay between structure and dynamics of complex networks using geometrical arguments. However, the field is still in its infancy. In this work we investigate the role of network geometry in determining the nature of the percolation transition in planar hyperbolic manifolds. Boettcher *et al.* [Nat. Comm. **3**, 787 (2012)] have shown that a special type of two-dimensional hyperbolic manifolds, the Farey graphs, display a discontinuous transition for ordinary link percolation. Here we investigate using the renormalization group the critical properties of link percolation on a wider class of two-dimensional hyperbolic deterministic and random manifolds constituting the skeletons of two-dimensional cell complexes. These hyperbolic manifolds are built iteratively by subsequently gluing m-polygons to single edges. We show that when the size m of the polygons is drawn from a distribution q_m with asymptotic power-law scaling $q_m \simeq Cm^{-\gamma}$ for $m \gg 1$, different universality classes can be observed depending on the value of the power-law exponent γ. Interestingly, the percolation transition is hybrid for $\gamma \in (3, 4)$ and becomes continuous for $\gamma \in (2, 3)$.

I. INTRODUCTION

The field of network topology and geometry is gaining increasing attention [1,2]. When modeling network geometry, higher-order networks such as simplicial and cell complexes are a natural choice [3–8]. Simplicial complexes are formed by simplices that describe the interaction between one, two, or more than two nodes, and they include nodes, links, triangles, and tetrahedra. Cell complexes are also formed by high-dimensional building blocks, but these building blocks can be any polytopes and do not need to be formed by a set of fully connected nodes. Models of simplicial and cell complexes growing by the subsequent addition of simplices and polytopes include Farey graphs [7], Apollonian networks [8], and the recently introduced Network Geometry with Flavor [3,4], which displays emergent hyperbolic network geometry [5]. The investigation of the relation between network geometry of simplicial complexes and dynamics is still in its infancy, and only recently have a few works been tackling problems in percolation [9], synchronization [10,11], and epidemic spreading [12]. These results significantly enrich the active debate on the role that hyperbolic networks have on navigability [13–15].

The interplay between hyperbolic network geometry and percolation [9,16–20] appears to be very profound. A classical result [17] of percolation states that in hyperbolic networks as well as in nonamenable graphs percolation exhibits two phase transitions: at the lower percolation threshold an infinite

cluster emerges but remains subextensive, and at the upper percolation threshold the infinite cluster becomes extensive. Even more interesting is the result of Boettcher, Singh, and Ziff [16], which shows that on the two-dimensional Farey graph, link (or bond) percolation is discontinuous. Finally, it has been shown in Ref. [9] that on simplicial complexes of dimension d one can define up to $2d$ topological percolation problems that can display a critical behavior that cannot be predicted by exclusively studying node and link percolation problems on the same network geometries.

Percolation is among the most widely studied critical phenomena on networks [21–29], and for many years it has been argued that percolation could lead to only second-order phase transitions. However, in recent years, there has been an increasing interest in unveiling the basic mechanisms responsible for abrupt percolation transitions in complex networks. In multiplex networks [30] it has been shown that interdependent percolation leads to hybrid phase transitions [30–33]. In simple networks it has been shown that network processes that are responsible for growing network structure can lead to abrupt but continuous phase transitions (explosive percolation) [34–37] as well as truly discontinuous phase transitions [38,39]. Moreover, it has been shown [40] that in the large deviation theory of percolation, discontinuous phase transitions can be observed if aggravating configurations of the initial damage are considered. In this context the result of Ref. [16] is revealing of the important interplay between

network geometry and the emergence of discontinuous critical behavior of percolation. Interestingly, the discontinuous nature of this link percolation transition is likely to be related to previous work on critical phenomena on one-dimensional systems with long-range interactions [41,42]. However this relation has so far not been clearly established.

In this work we address the question of the interplay between hyperbolic network geometry and percolation in dimension $d = 2$. In particular our goal is to explore how robust the discontinuity of link percolation observed in Farey graphs is with respect to modifications of the geometry of the building blocks of the planar hyperbolic manifold. Percolation on hierarchical lattices has been widely explored [43–47] in the literature, and advanced renormalization group (RG) techniques [48–52] have been developed for studying percolation and critical phenomena on hierarchical networks. Here we build on this literature to perform a comprehensive RG study of link percolation in deterministic and random hyperbolic manifolds in two dimensions. We show that when the size m of the polygons forming the random hyperbolic manifold is drawn from a distribution q_m with asymptotic power-law scaling $q_m \simeq Cm^{-\gamma}$ for $m \gg 1$, a rich scenario is observed with the occurrence of different universality classes depending on the power-law exponent γ.

The paper is organized as follows: in Sec. II we introduce the deterministic and the random hyperbolic manifolds studied in this paper; in Sec. III we introduce the main properties of percolation in hyperbolic networks including the upper and lower percolation thresholds and the fractal exponent; in Sec. III we determine the equation of the percolation probability, and we characterize its critical behavior; in Sec. IV we derive the expression for the generating function of the largest component; in Sec. V we determine the equations for the fractal exponent, and we characterize its critical behavior; in Sec. VI we determine the equations for the order parameter of percolation, and we establish the universality class of percolation at the upper critical threshold; finally in Sec. VII we provide the conclusions.

II. DETERMINISTIC AND RANDOM HYPERBOLIC MANIFOLDS

A. Deterministic hyperbolic manifolds

The deterministic manifolds considered in this paper are infinite hyperbolic simplicial complexes constructed deterministically and iteratively starting from a single link. At iteration $n = 0$ we attach an m-polygon (polygon with m links) to the initial link. At each iteration $n > 0$ we attach an m-polygon to every link introduced at iteration $n - 1$. At iteration n the number of nodes N_n and links L_n are given by

$$N_n = 1 + (m - 1)^n,$$
$$L_n = \frac{1}{m - 2}[(m - 1)^{n+1} - 1]. \tag{1}$$

The resulting networks constitute the 1-skeleton of $d = 2$ hyperbolic cell complexes and describe hyperbolic manifolds. In fact, they are 2-connected, and every link is incident at most to two polygons. These hyperbolic manifolds generalize the Farey graphs studied in Ref. [16], which correspond to
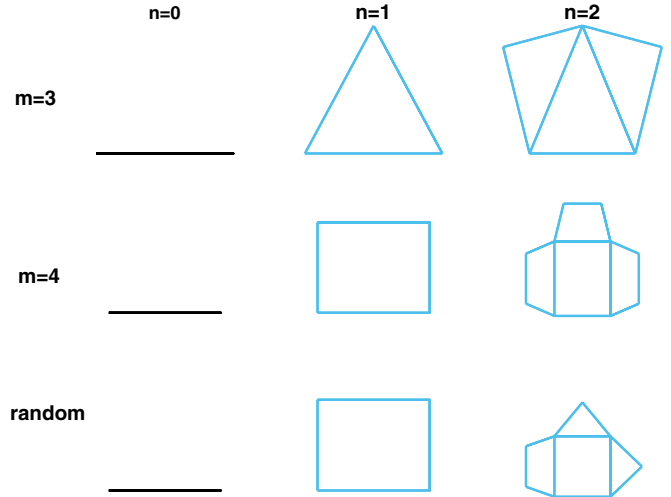

FIG. 1. The first iterations $n = 0$, $n = 1$, and $n = 2$ for the constructions of the considered hyperbolic manifolds are shown in the case in which the hyperbolic manifold is deterministic and formed only by triangles ($m = 3$) or squares ($m = 4$) and in the case in which the hyperbolic manifold is random with $q_m = 0.5\,\delta_{m,3} + 0.5\,\delta_{m,4}$.

the case $m = 3$, i.e., to the case in which the network is constructed by gluing subsequent triangles to links. In Fig. 1 we show the outcome of the first iterations generating the deterministic hyperbolic manifolds with $m = 3$ and $m = 4$ respectively.

B. Random hyperbolic manifolds

The random hyperbolic manifolds considered in this paper are constructed using an iterative procedure similar to the one used for constructing the deterministic hyperbolic manifolds considered above. However, the difference in their construction is that we allow the cell complexes to include polygons of different sizes m. To this end we consider an ensemble of random hyperbolic manifolds growing iteratively from a single link. At iteration $n = 0$ we draw a value of $m > 2$ from a distribution q_m, and we attach an m-polygon to the initial link. At iteration $n > 0$, for each link added at the previous iteration, we draw a value of $m > 2$ from a distribution q_m, and we attach an m-polygon to it.

In order to have a well-defined model of random hyperbolic manifolds we will assume here and in the following that the distribution q_m has a well-defined first moment $\langle m \rangle$. Under this hypothesis the expected number of nodes $\bar{N}_n$ and links $\bar{L}_n$ in the manifold at iteration n are given by

$$\bar{N}_n = 1 + (\langle m \rangle - 1)^n,$$
$$\bar{L}_n = \frac{1}{\langle m \rangle - 2}[(\langle m \rangle - 1)^{n+1} - 1]. \tag{2}$$

In Fig. 3 we show the outcome of the first iterations generating a random hyperbolic manifold in which we attach with equal probability either triangles or squares, i.e., $q_m = 0.5\,\delta_{m,3} + 0.5\,\delta_{m,4}$, where here and in following $\delta_{a,b}$ indicates the Kronecker delta. Note that the randomness of these hyperbolic manifolds is due only to the fact that we can add polygons of different number of links m. Therefore the random hyperbolic

manifolds reduce to the deterministic hyperbolic manifolds defined previously when the distribution $q_{m'}$ is given by $q_{m'} = \delta_{m,m'}$. Consequently the deterministic hyperbolic manifolds can also be called regular hyperbolic manifolds.

III. PERCOLATION IN HYPERBOLIC MANIFOLDS

In link percolation (also called bond percolation) links are removed with probability $f = 1 - p$, and the fraction P_∞ of nodes belonging to the giant component is studied as a function of p. However, in the considered hyperbolic manifolds percolation can also be characterized by the *percolation probability* T and the *fractal exponent* ψ. The percolation probability T indicates the probability that the two initial nodes present at iteration $n = 0$ are connected as $n \to \infty$ when links are removed with probability $f = 1 - p$. The fractal critical exponent ψ determines the size of the largest percolation cluster. In particular the study of T and ψ reveals that link percolation on hyperbolic manifolds [17] and in general nonamenable graphs has not just one but two percolation thresholds: the lower threshold $p^\star$ and the upper threshold p_c. Therefore, the phase diagram of link percolation on hyperbolic manifolds includes three regions:

(1) For $p < p^\star$ no cluster has infinite size. In this phase the percolation probability is null in the infinite network limit $n \to \infty$ (i.e., $T = 0$), indicating that the two initial nodes are not connected.

(2) For $p^\star < p < p_c$ the network has a nonzero probability $T > 0$ that the initial two nodes are connected. Moreover, in this phase the cluster that is connected to the initial two nodes at iteration n has an expected size R_n which is infinite (increases with the network size N_n) but subextensive. In other words, R_n scales with the expected total number of nodes $\bar{N}_n$ in the network as

$$R_n \sim \bar{N}_n^{\psi_n} \qquad (3)$$

with $0 < \psi_n < 1$ where the limit

$$\psi = \lim_{n \to \infty} \psi_n \qquad (4)$$

indicates the *fractal critical exponent*.

(3) For $p > p_c$ the network has an extensive cluster. In this case the probability that the initial two nodes are connected is one, i.e., $T = 1$, and the fraction P_∞ of nodes in the giant component scales like

$$P_\infty = \lim_{n \to \infty} \frac{R_n}{\bar{N}_n} = O(1), \qquad (5)$$

or equivalently $\psi = 1$.

IV. PERCOLATION PROBABILITY

A. Recursive equation for the percolation probability

Let us indicate with T_n the probability that the two nodes present at iteration $n = 0$ are connected at generation n. Given the iterative process that defines the hyperbolic manifold, it is easy to show that for the random-m case T_n satisfies the RG equation

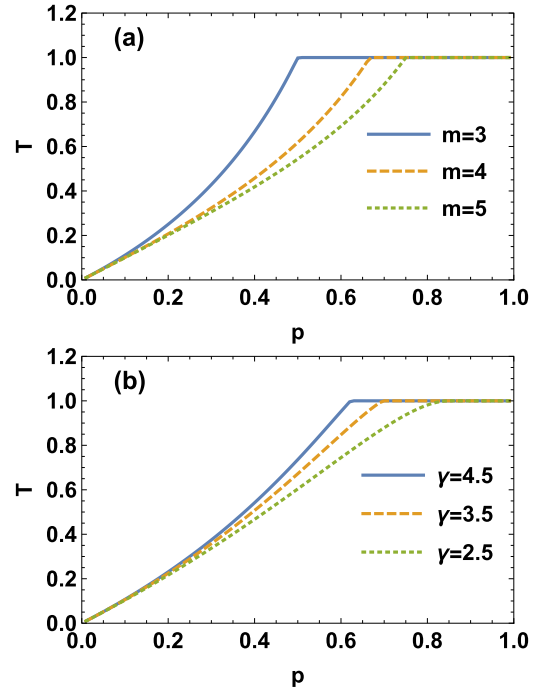$$T_{n+1} = p + (1 - p) \sum_{m=3}^{\infty} q_m T_n^{m-1} \qquad (6)$$

FIG. 2. The percolation probability T is plotted versus p for deterministic hyperbolic manifolds with $m = 3, 4, 5$ (a) and random hyperbolic manifolds with scale-free distribution $q_m = C m^{-\gamma}$ with $m \geq 3$ and $\gamma = 4.5, 3.5, 2.5$ (b).

with initial condition $T_0 = p$. If the link that directly connects the two initial nodes is not damaged, the two nodes are clearly connected. This event occurs with probability p. If the link that directly connects the initial two nodes is instead damaged (events that occur with probability $1 - p$), the two nodes are connected only if they are connected by a path that passes through each other node belonging to the polygon added at generation $n = 1$. Since the size the polygon added at iteration $n = 1$ has size m with probability q_m, the latter event occurs with probability $\sum_{m=3}^{\infty} q_m T_n^{m-1}$. For our further calculations it is useful to express Eq. (6) as

$$T_{n+1} = F(p, T_n), \qquad (7)$$

where

$$F(p, T_n) = p + (1 - p) Q(T_n), \qquad (8)$$

and where $Q(T)$ indicates the function

$$Q(T) = \sum_{m>2} q_m T^{m-1}. \qquad (9)$$

When the number of iterations n diverges $n \to \infty$ we observe that T_n converges to its limiting value T, i.e., $T_n \to T$, expressing the probability that the initial two nodes are connected in an infinite random hyperbolic manifold. Therefore, starting from the recursive Eq. (6) we obtain the implicit equation for T given by

$$T = p + (1 - p) Q(T). \qquad (10)$$

In Fig. 2 we show the linking probability T as a function of p for deterministic hyperbolic manifolds and random hyperbolic manifolds with scale-free distribution q_m. By studying the
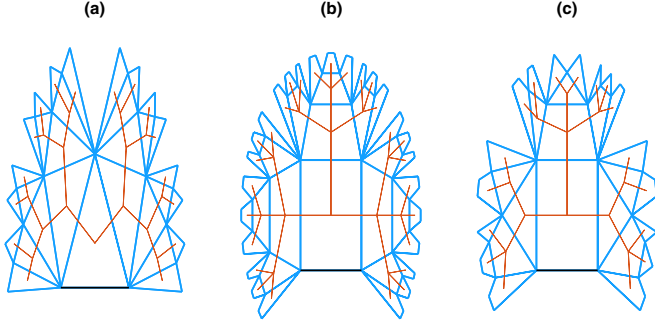
FIG. 3. The results of the first n iterations generating the regular hyperbolic manifolds with $m = 3$ (a) and $m = 4$ (b) are shown in blue (thick line), together with the results of the first n iteration generating a random hyperbolic manifold with $q_m = 1/2\,\delta(m, 3) + 1/2\,\delta(m, 4)$ (c). The initial link is indicated in black, and the dual network (the tree) is indicated in red (thin line). The number of iterations n is $n = 5$ for panel (a) and $n = 4$ for panels (b) and (c).

stability of the solutions $T^\star = 0$ and $T_c = 1$ we observe that Eq. (10) identifies the lower percolation threshold $p^\star$ and the upper percolation threshold p_c as

$$p^\star = 0, \quad T^\star = 0;$$

$$p_c = 1 - \frac{1}{\langle m \rangle - 1}, \quad T_c = 1.$$

For a deterministic hyperbolic manifold with $q_{m'} = \delta_{m,m'}$ we obtain then

$$p^\star = 0, \quad T^\star = 0;$$

$$p_c = 1 - \frac{1}{m - 1}, \quad T_c = 1.$$

It is interesting to compare these results to percolation on a Cayley tree with $m - 1$ descendants, which is the dual lattice to the manifolds considered here, as shown in Fig. 3. The probability of a bond presence on a dual lattice is $\tilde{p} = 1 - p$, and, indeed, the lower percolation threshold for the Cayley tree is known to be $1/(m - 1) = 1 - p_c$, where p_c is given by Eq. (11). In this case $T = 1 - S$, where S is the probability that a randomly chosen link in the dual tree leads to the giant component in the direction away from the root. However, there are no known connections between P_∞ and the properties of the dual lattice.

As a side note, we observe that the existence of the $T = T_c = 1$ solution of Eq. (10) is the necessary condition for the presence of an extensive component in the network, i.e., the presence of an upper percolation threshold p_c. Interestingly the presence of this phase at a nontrivial critical point $p = p_c < 1$ is not guaranteed in any modification of the hyperbolic manifold construction. In particular, if we modify the network construction by replacing the chain of $m - 1$ iterable links by one that has $m - 1 - k$ iterable links and k noniterable links we will construct a Cantor set structure. For this structure the linking probability would satisfy

$$T = p + (1 - p)p^k T^{m-1-k}, \quad (11)$$

and the $T = T_c = 1$ solution would not be allowed unless $p = p_c = 1$.

TABLE I. Mathematical mapping between the quantities determining the percolation probability T in the hyperbolic random manifold and the mathematical quantities determining the probability S' that by following a random link of a random network with degree distribution $P(k)$ we reach a node in the giant component.

Hyperbolic Random manifold	Random network
T	$1 - S'$
p	$1 - \tilde{p}$
m	k
q_m	$\frac{k}{\langle k \rangle} P(k)$
$\langle 1/m \rangle$	$\langle k \rangle_P$

B. Mapping to percolation of random networks

In this section we reveal that the critical behavior of T for $0 < p_c - p \ll 1$ can be nontrivial by considering a mapping between the Eq. (10) for T and percolation on random networks. In fact, Eq. (10) determines that the percolation probability T can be mapped to the equation for the probability S' that a random link reaches a node in the giant component of a random uncorrelated network with degree distribution $P(k)$ and minimum degree $k_{\min} \geqslant 3$. When nodes are damaged with probability $1 - \tilde{p}$ the equation for S' reads

$$S' = \tilde{p} \sum_k \frac{k}{\langle k \rangle_P} P(k)[1 - (1 - S')^{k-1}], \quad (12)$$

where $\langle k \rangle_P = \sum k P(k)$. Therefore at the mathematical level the equation determining T in random hyperbolic manifolds and the equation determining S' in a random network can be mapped to each other.

In this mapping the size of the polygon m corresponds to the degree of a node k, the probability distribution q_m corresponds to the distribution of excess degree $kP(k)/\langle k \rangle$, $\langle 1/m \rangle = \sum_m q_m/m$ corresponds to $\langle k \rangle_P$, and p corresponds to $1 - \tilde{p}$ (see Table I).

Note that finite random uncorrelated networks have the structural cutoff, i.e., the maximum degree $k_{\max}$ scales like the square root of the number of nodes in the network. However, in our mathematical mapping between Eq. (10) and Eq. (12) there is no prescribed mapping between the number of nodes in the random uncorrelated network and the number of nodes in the hyperbolic manifold; therefore the mapping described in this section can be performed for manifolds with an arbitrary large value of $m_{\max}$.

In this mapping the upper percolation threshold p_c maps to the well-known percolation threshold $\tilde{p}_c$ for the random network. In fact, we have that p_c is determined by the equation

$$(1 - p_c)\left[\sum_{m=3}^{\infty} q_m(m - 1)\right] = 1. \quad (13)$$

By substituting

$$1 - p_c \to \tilde{p}_c, \quad m \to k, \quad q_m \to \frac{k}{\langle k \rangle_P} P(k), \quad (14)$$

we obtain

$$\tilde{p}_c \left[\sum_{k>2} \frac{k(k-1)}{\langle k \rangle} P(k) \right] = 1 \quad (15)$$

or

$$\tilde{p}_c = \frac{\langle k \rangle_P}{\langle k^2 \rangle_P - \langle k \rangle_P}, \quad (16)$$

where the averages $\langle \ldots \rangle_P$ are over the distribution $P(k)$. It is well known that the percolation threshold and the critical behavior of percolation are strongly affected by power-law degree distributions for random networks, which display anomalous critical exponents [21,23–25,31]. For example, for the distribution $q_m \simeq C m^{-\gamma}$ for $m \gg 1$ and $\gamma \to 2^+$, the percolation threshold $p_c \to 1$. Therefore in this limit the network displays an extensive giant component only when the fraction of damaged nodes $f = 1 - p = 0$. This regime corresponds to the regime in which random networks have a degree distribution decaying as $P(k) \simeq C k^{-\tilde{\gamma}}$ with $\tilde{\gamma} \to 3^+$ and percolation threshold $\tilde{p}_c \to 0$.

C. Critical behavior of the linking probability

Using the mapping between random hyperbolic manifolds and random networks we can also determine the different critical behaviors for T in the deterministic and in the random hyperbolic manifolds. To this end we will consider different scenarios.

First, we consider the case of a generic distribution q_m displaying finite average moments $\langle m \rangle$ and $\langle m^2 \rangle$. This case clearly includes the deterministic hyperbolic manifold. For $0 < p_c - p \ll 1$ the function $Q(T)$ can be expanded in powers of $\Delta T = T - T_c$ as we have $|\Delta T| \ll 1$, yielding

$$Q(T) = 1 + (\langle m \rangle - 1)(\Delta T) + \frac{1}{2}\langle (m-1)(m-2) \rangle (\Delta T)^2 + o[(\Delta T)^2]. \quad (17)$$

Using this expansion in Eq. (10), we get

$$T = 1 - A(p_c - p)^\beta + o[(p_c - p)^\beta], \quad (18)$$

where the critical exponent β is given by

$$\beta = 1, \quad (19)$$

and where A is a constant given by

$$A = \frac{2(\langle m \rangle - 1)^2}{\langle (m-2)(m-1) \rangle}, \quad (20)$$

in particular, in the case of a deterministic hyperbolic manifold $A = A_m$ where A_m is given by

$$A_m = 2\frac{m-1}{m-2}. \quad (21)$$

Second, we consider the case of distributions q_m with power-law asymptotic behavior

$$q_m \simeq C m^{-\gamma}, \quad (22)$$

for $m \gg 1$ where the range of possible exponents is $\gamma \in (2, \infty]$ as we need to guarantee that $\langle m \rangle$ is finite as mentioned

TABLE II. Expansions of $T_c - T$ for $p = p_c - \epsilon$ and $0 < \epsilon \ll 1$. Here $\gamma > 2$ denotes the exponent of the asymptotic power-law scaling of the q_m distribution, i.e., $q_m \simeq C m^{-\gamma}$ for $m \gg 1$. For the case $\gamma = 3$ the critical exponent β is not defined (N/A) since the scaling of $T_c - T$ is linear with logarithmic corrections.

γ	Expansion of $T_c - T$	β
$\gamma > 3$	$A_\gamma(p_c - p)$	1
$\gamma = 3$	$A_\gamma(p_c - p)[-\ln(p_c - p)]^{-1}$	N/A
$2 < \gamma < 3$	$A_\gamma(p_c - p)^{\frac{1}{\gamma-2}}$	$\frac{1}{\gamma-2}$

above. Special attention is devoted in particular to power-law exponents $\gamma \leqslant 3$ corresponding to a diverging moment $\langle m^2 \rangle$. In particular in this regime, by following techniques already developed for random networks [21,23–25,31], we found a series of anomalous critical exponents.

(a) Case $\gamma > 3$

For $\gamma > 3$ both moments $\langle m \rangle$ and $\langle m^2 \rangle$ converge, so this case follows in the universality class of the case we have studied previously. Specifically in this case we can expand $Q(T)$ for $|\Delta T| \ll 1$ getting

$$Q(T) = 1 + (\langle m \rangle - 1)\Delta T + a_\gamma(\Delta T)^2 + o[(\Delta T)^2)] \quad (23)$$

with $a_\gamma = \langle (m-1)(m-2) \rangle / 2$ (see Table IV for its expression in the case of a pure power-law distribution q_m). By inserting this asymptotic expansion in Eq. (10) we obtain

$$T = 1 - A_\gamma(p_c - p)^\beta + o[(p_c - p)^\beta], \quad (24)$$

with $A_\gamma = \langle m - 1 \rangle / a_\gamma$ and

$$\beta = 1. \quad (25)$$

(b) Case $\gamma = 3$

For $\gamma = 3$ we can expand $Q(T)$ for $|\Delta T| \ll 1$ getting

$$Q(T) = 1 + \langle m - 1 \rangle \Delta T + a_\gamma(\Delta T)^2 \ln|\Delta T| O[(\Delta T)^2] \quad (26)$$

with a_γ indicating a constant (see Table IV for its expression in the case of a pure power-law distribution q_m). By inserting this asymptotic expansion in Eq. (10) we obtain

$$T = 1 - A_\gamma(p_c - p)[-\ln(p_c - p)]^{-1} + O(p_c - p), \quad (27)$$

with $A_\gamma = -(\langle m \rangle - 1)^2 / a_\gamma$.

(c) Case $\gamma \in (2, 3)$

For $\gamma \in (2, 3)$ we can expand $Q(T)$ for $|\Delta T| \ll 1$ getting

$$Q(T) = 1 + (\langle m \rangle - 1)\Delta T + a_\gamma|\Delta T|^{\gamma-1} + o(|\Delta T|^{\gamma-1}), \quad (28)$$

with a_γ indicating a constant (see Table IV for its expression in the case of a pure power-law distribution q_m). By inserting this asymptotic expansion in Eq. (10) we obtain

$$T = 1 - A_\gamma(p_c - p)^\beta + o[(p_c - p)^\beta], \quad (29)$$

with $A_\gamma = [(\langle m \rangle - 1)^2 / a_\gamma]^\beta$ and

$$\beta = \frac{1}{\gamma - 2}. \quad (30)$$

FIG. 4. Diagrammatic representation of generating functions $\hat{T}_n(x)$ (a) and $\hat{S}_n(x, y)$ (b). Filled areas indicate clusters that either connect $[\hat{T}_n(x)]$ or do not connect $[\hat{S}_n(x, y)]$ the end nodes.

In Table II we summarize the different scaling behaviors observed for different values of γ.

V. GENERATING FUNCTIONS FOR FINITE COMPONENTS

A. General framework

In order to fully characterize the percolation transition in the considered hyperbolic manifolds we follow the theoretical approach proposed by Boettcher *et al.* [16], and we investigate the properties of the generating functions $\hat{T}_n(x)$ and $\hat{S}_n(x, y)$. In the hyperbolic manifolds obtained at iteration n the function $\hat{T}_n(x)$ is the generating function of the number of nodes in the connected component linked to both initial nodes. The function $\hat{S}_n(x, y)$ is the generating function for the sizes of the two connected components linked exclusively to one of the two initial nodes. These generating functions can be expressed as

$$\hat{T}_n(x) = \sum_{\ell=0}^{\infty} t_n(\ell) x^\ell,$$

$$\hat{S}_n(x, y) = \sum_{\ell, \bar{\ell}} s_n(\ell, \bar{\ell}) x^\ell y^{\bar{\ell}}, \tag{31}$$
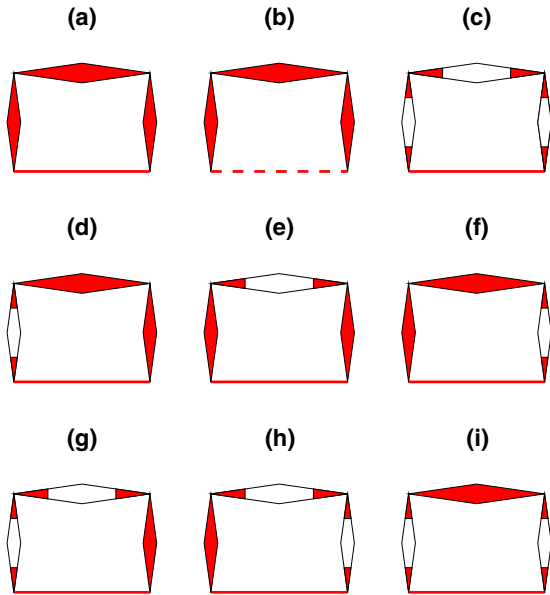

FIG. 5. The diagrams contributing to $\hat{T}_{n+1}(x)$ for the deterministic manifold with $m = 4$ are shown. The contributions from configurations (a), (b), and (d)–(h) are $px^2\hat{T}_n^3(x)$ (a), $(1-p)x^2\hat{T}_n^3(x)$ (b), $px^2\hat{T}_n^2(x)\hat{S}_n(x, x)$ (d–f), $px\hat{T}_n(x)\hat{S}_n^2(x, 1)$ (g, h). The comprehensive contribution of configurations (c) and (i) is $\hat{S}_n^2(x, 1)$.
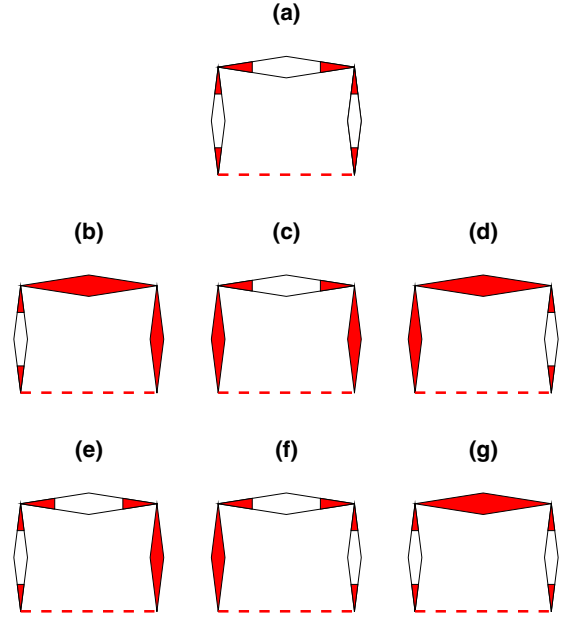

FIG. 6. The diagrams contributing to $\hat{S}_{n+1}(x)$ for the deterministic manifold with $m = 4$ are shown. The comprehensive contribution from configurations (a) and (g) is $(1-p)\hat{S}_n(x, 1)\hat{S}_n(y, 1)$. The contributions from the other configurations are $(1-p)y^2\hat{T}_n^2(y)\hat{S}_n(x, y)$ (b), $(1-p)xy\hat{T}_n(x)\hat{T}_n(y)\hat{S}_n(x, y)$ (c), $(1-p)x^2\hat{T}_n^2(x)\hat{S}_n(x, y)$ (d), $(1-p)y\hat{T}_n(y)\hat{S}_n(x, 1)\hat{S}_n(y, 1)$ (e), $(1-p)x\hat{T}_n(x)\hat{S}_n(x, 1)\hat{S}_n(y, 1)$ (f).

where $t_n(\ell)$ indicates the distribution of the number of nodes ℓ connected to the two initial nodes and $s_n(\ell, \bar{\ell})$ indicates the joint distribution of the number of nodes ℓ connected exclusively to a given initial node and the number of nodes $\bar{\ell}$ connected exclusively to the other initial node.

The size R_n of the connected component linked to the initial two nodes at iteration n is given by

$$R_n = \left. \frac{d\hat{T}_n(x)}{dx} \right|_{x=1}. \tag{32}$$

By explicitly deriving R_n it can be shown that for $n \gg 1$, R_n scales like

$$R_n \sim \bar{N}_n^\psi, \tag{33}$$

with $\psi \in (0, 1]$ for $p > p^\star$. In the section below we will consider the recursive equation that can be used to determine the generating functions $\hat{T}_n(x)$ and $\hat{S}_n(x, y)$ for the deterministic and the random hyperbolic manifolds, while the next section will be devoted to the evaluation of the fractal exponent ψ.

B. Deterministic hyperbolic manifold

Here we establish the equations determining the generating functions $\hat{T}_n(x)$ and $\hat{S}_n(x, y)$ for the deterministic hyperbolic manifold formed by gluing m-polygons together. These recursive equations for $\hat{T}_n(x)$ and $\hat{S}_n(x, y)$

start from the initial condition $T_0(x) = 1 - \hat{S}_0(x, y) = p$ and read

$$\hat{T}_{n+1}(x) = p\left[x^{m-2}\hat{T}_n^{m-1}(x) + (m-1)x^{m-2}\hat{T}_n^{m-2}(x)\hat{S}_n(x, x) + \sum_{i=0}^{m-3}(i+1)x^i\hat{T}_n^i(x)\hat{S}_n^2(x, 1) \right] + (1-p)x^{m-2}\hat{T}_n^{m-1}(x),$$

$$\hat{S}_{n+1}(x, y) = (1-p)\left[\sum_{i=0}^{m-2}x^i y^{m-2-i}\hat{T}_n^i(x)\hat{T}_n^{m-2-i}(y)\hat{S}_n(x, y) + \sum_{i=0}^{m-3}\sum_{j=0}^{m-3-i}x^i y^j\hat{T}_n^i(x)\hat{T}_n^j(y)\hat{S}_n(x, 1)\hat{S}(1, y) \right]. \tag{34}$$

The generating function $\hat{T}_{n+1}(x)$ of the size of the connected component joining the two initial nodes should consider only contributions from configurations in which the link that connects the two initial nodes is not damaged, or the cases in which the initial link is damaged but the two initial nodes are connected through paths that pass through each other node of the m-polygon added at iteration $n = 1$. The generating function $\hat{S}_{n+1}(x, y)$ should instead take into account only contributions from configurations in which the initial link between the two initial nodes is damaged and there exists no alternative path connecting the two initial nodes.

In order to derive these equations it is possible to consider the simple cases in which $m = 3$ and $m = 4$ and by induction prove the general formula for a generic value of m. The recursive equations for $m = 3$ and 4 can be easily derived diagrammatically using the diagram for $\hat{T}_n(x)$ and $\hat{S}_n(x, y)$ shown in Fig. 4. For the case $m = 3$ these equations reduce to the equations derived in Ref. [16] for the Farey graph, which read

$$\hat{T}_{n+1}(x) = p\{x\hat{T}_n^2(x) + 2x\hat{T}_n(x)\hat{S}_n(x, x) + \hat{S}_n(1, x)\hat{S}_n(1, x)\} + (1-p)x\hat{T}_n^2(x),$$

$$\hat{S}_{n+1}(x, y) = (1-p)\{x\hat{T}_n(x)\hat{S}_n(x, y) + y\hat{S}_n(x, y)\hat{T}_n(y) + \hat{S}_n(x, 1)\hat{S}_n(y, 1)\}. \tag{35}$$

In the case $m = 4$ instead the equations can be derived by using a diagrammatic representation of the configurations that contribute to $\hat{T}_{n+1}(x)$ and $\hat{S}_{n+1}(x, y)$ (see Figs. 5 and 6) obtaining

$$\hat{T}_{n+1}(x) = p\left[x^2\hat{T}_n^3(x) + 3x^2\hat{T}_n^2(x)\hat{S}_n(x, x) + 2x\hat{T}_n(x)\hat{S}_n(x, 1)\hat{S}_n(x, 1) + \hat{S}_n(x, 1)\hat{S}_n(x, 1) \right] + (1-p)x^2\hat{T}_n^3(x),$$

$$\hat{S}_{n+1}(x, y) = (1-p)\left[x^2\hat{T}_n^2(x)\hat{S}_n(x, y) + y^2\hat{T}_n^2(y)\hat{S}_n(x, y) + xy\hat{T}_n(x)\hat{S}_n(x, y)\hat{T}_n(y) + x\hat{T}_n(x)\hat{S}_n(x, 1)\hat{S}_n(y, 1) \right.$$

$$\left. + y\hat{T}_n(y)\hat{S}_n(y, 1)\hat{S}_n(x, 1) + \hat{S}_n(x, 1)\hat{S}_n(y, 1) \right]. \tag{36}$$

C. Random hyperbolic manifolds

The recursive equations for the generating functions $\hat{T}_n(x)$ and $\hat{S}_n(x, y)$ of the random hyperbolic manifold can be easily derived from the Eqs. (34) for the same generating function in a deterministic m-polygon hyperbolic manifolds by averaging over the distribution q_m. In this way we obtain

$$\hat{T}_{n+1}(x) = \sum_{m=3}^{\infty} q_m\left[x^{m-2}\hat{T}_n^{m-1}(x) + p(m-1)x^{m-2}\hat{T}_n^{m-2}(x)\hat{S}_n(x, x) + p\sum_{i=0}^{m-3}(i+1)x^i\hat{T}_n^i(x)\hat{S}_n^2(x, 1) \right],$$

$$\hat{S}_{n+1}(x, y) = (1-p)\sum_{m=3}^{\infty} q_m\left[\sum_{i=0}^{m-2}x^i y^{m-2-i}\hat{T}_n^i(x)\hat{T}_n^{m-2-i}(y)\hat{S}_n(x, y) + \sum_{i=0}^{m-3}\sum_{j=0}^{m-3-i}x^i y^j\hat{T}_n^i(x)\hat{T}_n^j(y)\hat{S}_n(x, 1)\hat{S}_n(1, y) \right], \tag{37}$$

where $T_0(x) = 1 - \hat{S}_0(x, y) = p$. Notice that Eqs. (38) reduce to Eqs. (34) for a deterministic hyperbolic manifold formed by m' polygons for $q_{m'} = \delta_{m,m'}$.

VI. FRACTAL EXPONENT

A. General derivation

In this section we investigate how the expected size R_n of the giant component connected to the two initial nodes grows with the number of generations n, and from this expression we will derive the fractal exponent ψ. The expected size of the giant component R_n can be derived from the generating function $\hat{T}_n(x)$ by differentiation:

$$R_n = \left. \frac{d\hat{T}_n(x)}{dx} \right|_{x=1}. \tag{38}$$

To this end we rewrite Eqs. (38) in terms of the vector

$$\mathbf{V}_n(x) = \left(V_n^1(x), V_n^2(x), V_n^3(x) \right)^\top$$

$$= (\hat{T}_n(x), \Sigma_n(x), S_n(x))^\top, \tag{39}$$

where $\Sigma_n(x) = \hat{S}_n(x, x)$ and $S_n(x) = \hat{S}(1, x)$, obtaining a recursive equation of the type

$$\mathbf{V}_{n+1}(x) = \mathbf{F}_n(\mathbf{V}_n(x), x). \tag{40}$$

This system of equations can be differentiated obtaining

$$\frac{d\mathbf{V}_{n+1}(x)}{dx} = \sum_{s=1}^{3} \frac{\partial \mathbf{F}_n}{\partial V_n^s(x)}\frac{dV_n^s(x)}{dx} + \frac{\partial \mathbf{F}_n}{\partial x}, \tag{41}$$

with initial condition $\mathbf{V}_0' = (0, 0, 0)$ (the initial nodes are not counted). Since the nonhomogeneous term $\partial \mathbf{F}_n/\partial x$ is

subleading with respect to the homogeneous one, for $n \gg 1$ and $T < 1$ we have

$$\dot{\mathbf{V}}_{n+1} \simeq \mathcal{D}_n \prod_{n'=1}^{n} \lambda_{n'} \mathbf{u}_n, \tag{42}$$

where λ_n and $\mathbf{u}_n$ are the largest eigenvalue and the the corresponding eigenvector of the Jacobian matrix $\mathbf{J}_n$ defined as

$$[J_n]_{ij} = \frac{\partial F^i(x)}{\partial V^j(x)}\bigg|_{\mathbf{V}(x)=\mathbf{V}_n(1); x=1}, \tag{43}$$

and $\mathcal{D}_n$ is given by

$$\mathcal{D}_n = \left(\prod_{n'=2}^{n} \langle \mathbf{u}_{n'} | \mathbf{u}_{n'-1} \rangle \right) \langle \mathbf{u}_1 | \dot{\mathbf{V}}_0 \rangle, \tag{44}$$

with $\dot{\mathbf{V}}_0 = \partial \mathbf{F}_0 / \partial x$. Assuming that for $p \simeq p_c$, $\mathcal{D}_n$ is in first approximation independent of n, it follows that $R_n = \dot{V}_n^1$ scales like

$$R_n \sim \prod_{n'=1}^{n} \lambda_{n'} = \exp \left[\sum_{n'=0}^{n} \ln \lambda_n \right]. \tag{45}$$

By defining ψ_n as

$$\psi_n = \frac{\ln \lambda_n}{\ln(\langle m \rangle - 1)} \tag{46}$$

and using the expression for $\bar{N}_n$ given by Eq. (2) we get for $n \gg 1$

$$R_n \sim \bar{N}_n^{\psi}, \tag{47}$$

where the fractal exponent ψ is given by

$$\psi = \lim_{n \to \infty} \psi_n. \tag{48}$$

B. Deterministic and random hyperbolic manifolds

Here we will perform the explicit calculation outlined in the previous subsection by treating explicitly the random hyperbolic manifolds. In fact, the results for the deterministic hyperbolic manifolds can be deduced from these calculations by considering a distribution q_m equal to a Kronecker delta. The recursive equations for $\hat{T}_n(x)$, $\Sigma_n(x)$ and $S_n(x)$ can be directly deduced from Eqs. (38) by setting $y = x$ and $y = 1$ and using $\hat{T}_n(1) = 1 - \Sigma_n(1, 1) = 1 - S_n(1) = T_n$ and read

$$\hat{T}_{n+1}(x) = \sum_{m=3}^{\infty} q_m \left\{ x^{m-2} \hat{T}_n^{m-1}(x) + p(m-1)x^{m-2}\hat{T}_n^{m-2}(x)\Sigma_n(x) + p\left[\sum_{i=0}^{m-3} (i+1)x^i \hat{T}_n^i(x) \right] S_n^2(x) \right\},$$

$$\Sigma_{n+1}(x) = (1-p) \sum_{m=3}^{\infty} q_m \left\{ (m-1)x^{m-2}\hat{T}_n^{m-2}(x)\Sigma_n(x) + \left[\sum_{i=0}^{m-3} (i+1)x^i \hat{T}_n^i(x) \right] S_n^2(x) \right\},$$

$$S_{n+1}(x) = (1-p) \sum_{m=3}^{\infty} q_m \left[\sum_{i=0}^{m-2} x^i \hat{T}_n^i(x) \right] S_n(x). \tag{49}$$

By differentiating Eqs. (49) with respect to $\mathbf{V}_n$ and putting $x = 1$, and using $\hat{T}_n(1) = 1 - \Sigma_n(1, 1) = 1 - S_n(1) = T_n$, we get the Jacobian $\mathbf{J}_n$. In particular by using the mathematical relation

$$(1 - T_n) \sum_{i=0}^{m-3} i(i+1)T_n^{i-1} = 2 \sum_{i=0}^{m-3} (i+1)T_n^i - (m-1)(m-2)T_n^{m-3} \tag{50}$$

and

$$(1 - T_n) \sum_{i=0}^{m-3} (i+1)T_n^i = \sum_{i=0}^{m-2} T_n^i - (m-1)T_n^{m-2},$$

one can show that the Jacobian $\mathbf{J}_n$ can be expressed as

$$\mathbf{J}_n = \begin{pmatrix} Q'(T_n) + 2p[\mathrm{H}(T_n) - Q'(T_n)] & pQ'(T_n) & 2p[\mathrm{H}(T_n) - Q'(T_n)] \\ 2(1-p)[\mathrm{H}(T_n) - Q'(T_n)] & (1-p)Q'(T_n) & 2(1-p)[\mathrm{H}(T_n) - Q'(T_n)] \\ (1-p)[\mathrm{H}(T_n) - Q'(T_n)] & 0 & (1-p)\mathrm{H}(T_n) \end{pmatrix}, \tag{51}$$

where $Q(T)$ is defined in Eq. (9) and $H(T)$ is defined as

$$H(T) = \sum_{m=3}^{\infty} q_m \sum_{i=0}^{m-2} T^i, \tag{52}$$

which admits for $T < 1$ the expression

$$H(T) = \frac{1 - Q(T)}{1 - T}. \tag{53}$$

Similarly it can be shown that $\partial \mathbf{F}_n / \partial x$ is given by

$$\frac{\partial \mathbf{F}_n}{\partial x} = \begin{pmatrix} pT_n 2[H(T_n) - Q'(T_n)] + [T_n Q'(T_n) - Q(T_n)] \\ 2(1-p)T_n[H(T_n) - Q'(T_n)](1-p)T_n[H(T_n) - Q'(T_n)] \end{pmatrix}.$$

For $T_n < 1$ the Jacobian $\mathbf{J}_n$ has the largest eigenvalue λ_n given by

$$\lambda_n = \tfrac{1}{2}[\sqrt{\hat{\Delta}(T_n)} + \hat{K}(T_n)], \tag{54}$$

where $\hat{\Delta}(T_n)$ and $\hat{K}(T_n)$ are given by

$$\hat{\Delta}(T_n) = [\hat{K}(T_n)]^2 - 4(1-p)H(T_n)Q'(T_n),$$
$$\hat{K}(T_n) = (p+1)H(T_n) + (1-2p)Q'(T_n). \tag{55}$$

For $T_n = 1$, instead, the largest eigenvalue is given by

$$\lambda_n = \langle m \rangle - 1.$$

The eigenvector $\mathbf{u}_n$ corresponding to the largest eigenvalue is

$$\mathbf{u}_n = \mathcal{C} \begin{pmatrix} \hat{K}(T_n) - 2(1-p)H(T_n) + \sqrt{\hat{\Delta}(T_n)} \\ 4(1-p)[H(T_n) - Q'(T_n)] \\ 2(1-p)[H(T_n) - Q'(T_n)] \end{pmatrix}, \tag{56}$$

where $\mathcal{C}$ is the normalization constant. For $T_n = 1$ and $p = p_c$, the eigenvector $\mathbf{u}_n$ is given by

$$\mathbf{u}_n = (1, 0, 0)^\top.$$

In Fig. 7 we show the fractal exponent ψ_n as a function of p for deterministic hyperbolic manifolds with $m = 3, 4, 5$ and for $n = 1000$.

C. Scaling of the fractal exponent

The fractal exponent ψ is defined as the limit for $n \to \infty$ of ψ_n related to the maximum eigenvalue λ_n of the Jacobian
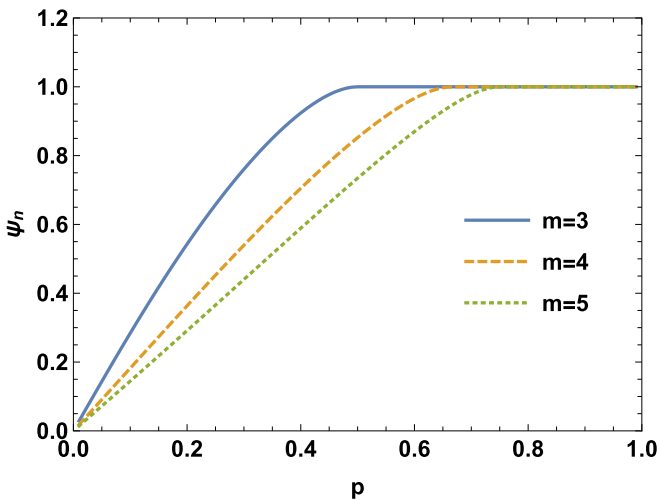

FIG. 7. The exponent ψ_n is shown as a function of p for the deterministic hyperbolic manifold with $m = 3, 4, 5$. All curves are obtained for $n = 1000$.

matrix $\mathbf{J}_n$ by Eq. (46). Since λ_n is expressed in Eq. (54) in terms of $Q'(T_n)$ and $H(T_n)$, by expanding these latter quantities for $0 < T_c - T_n \ll 1$ and $0 < p_c - p \ll 1$ we can derive the critical behavior of ψ_n that can be expressed as a function of $\Delta T_n = T_n - 1$:

$$\psi_n = f(\Delta T_n). \tag{57}$$

From this scaling, by performing the limit $n \to \infty$, we can derive the critical scaling of the fractal exponent. In the following we will analyze the critical behavior of ψ for distributions q_m with convergent first, second, and third moments $\langle m \rangle$, $\langle m^2 \rangle$, and $\langle m^3 \rangle$ and with asymptotic power-law scaling $q_m \simeq Cm^{-\gamma}$ with $\gamma > 2$. In particular we will show that for hyperbolic manifolds with scale-free distribution q_m the critical behavior becomes dependent on the exponent γ as summarized in Table III.

1. Case with converging $\langle m \rangle$, $\langle m^2 \rangle$, and $\langle m^3 \rangle$

The first case we consider is the case of a generic distribution q_m having convergent first, second, and third moments $\langle m \rangle$, $\langle m^2 \rangle$, and $\langle m^3 \rangle$. By expanding $Q'(T_n)$ and $H(T_n)$ close to the critical point, i.e., for $p = p_c + \Delta p$, and $T_n = T_c + \Delta T_n$ for $\Delta p < 0$ and $\Delta T_n < 0$ but small in absolute values, i.e., $|\Delta T_n| \ll 1$ and $|\Delta p| \ll 1$, we obtain

$$Q'(T_n) = (\langle m \rangle - 1) + \langle (m-1)(m-2) \rangle \Delta T_n$$
$$+ \tfrac{1}{2} \langle (m-1)(m-2)(m-3) \rangle (\Delta T_n)^2 + o[(\Delta T_n)^2],$$

$$H(T_n) = (\langle m \rangle - 1) + \tfrac{1}{2} \langle (m-1)(m-2) \rangle \Delta T_n$$
$$+ \tfrac{1}{6} \langle (m-1)(m-2)(m-3) \rangle (\Delta T_n)^2 + o[(\Delta T_n)^2].$$

Therefore by using the definition of ψ_n [Eq. (46)] and the explicit expression of λ_n [Eq. (54)] we can derive the scaling of ψ_n as a function of ΔT_n,

$$\psi_n = 1 - \hat{A}(\Delta T_n)^2 + o[(\Delta T_n)^2],$$

TABLE III. Asymptotic expansion of $1 - \psi_n$ and $1 - \psi$ in $\Delta T_n = T_n - 1$ and in $\Delta p = p - p_c$ valid for $\Delta p \ll 1$ and $|\Delta T_n| \ll 1$. Here we consider random hyperbolic manifolds with asymptotic power-law scaling of the q_m distribution, i.e., $q_m \simeq Cm^{-\gamma}$ for $m \gg 1$.

γ	Expansion of $1 - \psi_n$	Expansion of $1 - \psi$
$\gamma > 4$	$\hat{A}_\gamma (\Delta T_n)^2$	$\tilde{A}_\gamma (\Delta p)^2$
$\gamma = 4$	$\hat{A}_\gamma (\Delta T_n)^2 \ln|\Delta T_n|$	$\tilde{A}_\gamma (\Delta p)^2 \ln|\Delta p|$
$\gamma \in (3, 4)$	$\hat{A}_\gamma |\Delta T_n|^{\gamma-2}$	$\tilde{A}_\gamma |\Delta p|^{\gamma-2}$
$\gamma = 3$	$\hat{A}_\gamma \Delta T_n \ln|\Delta T_n|$	$\tilde{A}_\gamma \Delta p[\ln|\Delta p|]^2$
$\gamma \in (2, 3)$	$\hat{A}_\gamma |\Delta T_n|^{\gamma-2}$	$\tilde{A}_\gamma |\Delta p|$

where the constant $\hat{A}$ is given by

$$\hat{A} = \frac{3\langle(m-1)(m-2)\rangle + (\langle m \rangle - 1)(\langle m \rangle - 2)[\langle(m-1)(m-2)(m-3)\rangle]}{6(\langle m \rangle - 1)^2(\langle m \rangle - 2)\ln(\langle m \rangle - 1)}. \tag{58}$$

Specifically in the case in of a deterministic hyperbolic manifold, when $q_{m'} = \delta_{m',m}$, we have $\hat{A} = \hat{A}_m$ given by

$$\hat{A}_m = \frac{1}{6}\frac{m(m-2)}{\ln(m-1)}. \tag{59}$$

In order to derive the scaling of the fractal exponent ψ with Δp we use the fact that for $p_c - p \ll 1$ and $n \to \infty$ we have that $\Delta T = T - T_c$ is proportional to Δp with proportionality constant A [see Eq. (18)]. Therefore we predict that close to the critical point, for $0 < \Delta p \ll 1$, ψ is given by

$$\psi = 1 - \tilde{A}(p_c - p)^2 + o[(p_c - p)^2], \tag{60}$$

where

$$\tilde{A} = \frac{2(\langle m \rangle - 1)^2}{3[\langle(m-1)(m-2)\rangle]^2}\frac{3\langle(m-1)(m-2)\rangle + (\langle m \rangle - 1)(\langle m \rangle - 2)[\langle(m-1)(m-2)(m-3)\rangle]}{[\langle m \rangle - 2)\ln(\langle m \rangle - 1]}. \tag{61}$$

For a deterministic hyperbolic manifold with $q_{m'} = \delta_{m',m}$ with $m \geqslant 3$ the constant $\tilde{A}$ equals $\tilde{A}_m$, where

$$\tilde{A}_m = \frac{2m(m-1)^2}{3(m-2)\ln(m-1)}. \tag{62}$$

Interestingly, $\tilde{A}_m$ gains its minimum value at $m = 4$, which indicates that among this class of hyperbolic manifolds, the square hyperbolic manifold features the slowest conversion convergence of ψ to 1.

2. Case with power-law distribution q_m with power-law exponent γ

Here we consider the scaling of ψ_n as a function of ΔT_n and the scaling of the fractal exponent ψ as a function of Δp for random hyperbolic manifolds with asymptotic power-law distribution $q_m \simeq Cm^{-\gamma}$ as a function of the the value of the power-law exponent γ.

(1) Case $\gamma > 4$

This case reduces to the case of the generic distribution q_m having finite first, second, and third moments $\langle m \rangle$, $\langle m^2 \rangle$, and $\langle m^3 \rangle$ convergent, studied in the precedent subsection. In fact in this case we can expand the functions $Q'(T)$ and $H(T)$ for $\Delta p < 0$ and $\Delta T_n < 0$, with $|\Delta T_n| \ll 1$ and $|\Delta p| \ll 1$, getting

$$Q'(T_n) = (\langle m \rangle - 1) + \langle(m-1)(m-2)\rangle\Delta T_n + c_\gamma(\Delta T_n)^2$$
$$+ o[(\Delta T_n)^2],$$

$$H(T_n) = (\langle m \rangle - 1) + \frac{1}{2}\langle(m-1)(m-2)\rangle\Delta T_n + d_\gamma(\Delta T_n)^2$$
$$+ o[(\Delta T_n)^2],$$

where $c_\gamma = \langle(m-1)(m-2)(m-3)\rangle/2$ and $d_\gamma = \langle(m-1)(m-2)(m-3)\rangle/6$ (see Table IV for their expression in the case of a pure power-law distribution q_m). Using these expressions in Eq. (54) for λ_n we derive the critical scaling of ψ_n given by

$$\psi_n = 1 - \hat{A}_\gamma(\Delta T_n)^2 + o[(\Delta T_n)^2], \tag{63}$$

with $\hat{A}_\gamma = \hat{A}$ given by Eq. (58). Moreover in the limit $n \to \infty$ we predict that the fractal exponent ψ has critical behavior

$$\psi = 1 - \tilde{A}_\gamma(\Delta p)^2 + o[(\Delta p)^2], \tag{64}$$

with $\tilde{A}_\gamma = \tilde{A}$ given by Eq. (61).

(2) Case $\gamma = 4$

In this case we can perform the asymptotic expansion of $Q'(T_n)$ and $H(T_n)$ for $|\Delta T_n| \ll 1$ for $\Delta p < 0$ and $\Delta T_n < 0$ with $|\Delta T_n| \ll 1$ and $|\Delta p| \ll 1$ obtaining

$$Q'(T_n) = (\langle m \rangle - 1) + \langle(m-1)(m-2)\rangle\Delta T_n$$
$$+ c_\gamma(\Delta T_n)^2 \ln|\Delta T_n| + O[(\Delta T_n)^2],$$

$$H(T_n) = (\langle m \rangle - 1) + \frac{1}{2}\langle(m-1)(m-2)\rangle\Delta T_n$$
$$+ d_\gamma(\Delta T_n)^2 \ln|\Delta T_n| + O[(\Delta T_n)^2], \tag{65}$$

where c_γ and d_γ are constants (see Table IV for their expression in the case of a pure power-law distribution q_m). By inserting these asymptotic expansions in λ_n [given by Eq. (54)] we can derive the asymptotic expansion of ψ_n,

$$\psi_n = 1 - \hat{A}_\gamma(\Delta T_n)^2 \ln|\Delta T_n| + O(|\Delta T_n|^2), \tag{66}$$

where

$$\hat{A}_\gamma = \frac{c_\gamma - 2d_\gamma}{(\langle m \rangle - 1)\ln(\langle m \rangle - 1)}. \tag{67}$$

By performing the limit $n \to \infty$ and using the fact that close to the upper percolation threshold, Eq. (24) holds, we can easily show that the fractal exponent ψ scales like

$$\psi = 1 - \tilde{A}_\gamma(\Delta p)^2 \ln|\Delta p| + O(|\Delta p|^2), \tag{68}$$

where $\tilde{A}_\gamma = \hat{A}_\gamma A_\gamma^2$.

TABLE IV. Values of a_γ, c_γ, and d_γ determining, respectively, the asymptotic expansion of $Q(T)$, $Q'(T)$, and $H(T)$ for a pure power-law q_m distribution given by $q_m = Cm^{-\gamma}$, for $m \geqslant 3$.

γ	a_γ	c_γ	d_γ
$\gamma \geqslant 4$	$\frac{\zeta(\gamma-2)-3\zeta(\gamma-1)+2\zeta(\gamma)}{2(-1-2^{-\gamma}+\zeta(\gamma))}$	$\frac{360}{765-8\pi^4}$	$\frac{120}{765-8\pi^4}$
$\gamma \in (3,4)$	$\frac{\zeta(\gamma-2)-3\zeta(\gamma-1)+2\zeta(\gamma)}{2(-1-2^{-\gamma}+\zeta(\gamma))}$	$\frac{2^\gamma(\gamma-1)\Gamma[1-\gamma]}{-1-2^\gamma+2^\gamma\zeta(\gamma)}$	$\frac{2^\gamma\Gamma[1-\gamma]}{1+2^\gamma-2^\gamma\zeta(\gamma)}$
$\gamma = 3$	$\frac{4}{9-8\zeta(3)}$	$\frac{4}{9-8\zeta(3)}$	$\frac{4}{9-8\zeta(3)}$
$\gamma \in (2,3)$	$\frac{2^\gamma\Gamma[1-\gamma]}{-1-2^\gamma+2^\gamma\zeta(\gamma)}$	$\frac{2^\gamma(\gamma-1)\Gamma[1-\gamma]}{-1-2^\gamma+2^\gamma\zeta(\gamma)}$	$\frac{2^\gamma\Gamma[1-\gamma]}{1+2^\gamma-2^\gamma\zeta(\gamma)}$

(3) Case $\gamma \in (3, 4)$

In this case we consider the asymptotic expansion of $Q'(T_n)$ and $H(T_n)$ for $\Delta p < 0$ and $\Delta T_n < 0$ with $|\Delta T_n| \ll 1$ and $|\Delta p| \ll 1$ given by

$$Q'(T_n) = (\langle m \rangle - 1) + \langle (m-1)(m-2) \rangle \Delta T_n + c_\gamma |\Delta T_n|^{\gamma-2}$$
$$+ o(|\Delta T_n|^{\gamma-2}),$$

$$H(T_n) = (\langle m \rangle - 1) + \tfrac{1}{2} \langle (m-1)(m-2) \rangle \Delta T_n + d_\gamma |\Delta T_n|^{\gamma-2}$$
$$+ o(|\Delta T_n|^{\gamma-2}),$$

where c_γ and d_γ are constants (see Table IV for their expression in the case of a pure power-law distribution q_m). By following the same procedure applied to the previous case we obtain the asymptotic scaling for ψ_n given by

$$\psi_n = 1 - \hat{A}_\gamma |\Delta T_n|^{\gamma-2} + o(|\Delta T_n|^{\gamma-2}), \tag{69}$$

where A_γ is given by Eq. (67).
Finally performing the limit $n \to \infty$ and using Eq. (24) we derive the following asymptotic expansion for the fractal exponent ψ:

$$\psi = 1 - \tilde{A}_\gamma |\Delta p|^{\gamma-2} + o(|\Delta p|^{\gamma-2}), \tag{70}$$

where $\tilde{A}_\gamma = \hat{A}_\gamma A_\gamma^{(\gamma-2)}$.

(4) Case $\gamma = 3$

For $\gamma = 3$ we consider the asymptotic expansion of $Q'(T)$ and $H(T)$ for $\Delta p < 0$ and $\Delta T_n < 0$ with $|\Delta T_n| \ll 1$ and $|\Delta p| \ll 1$, which is given by

$$Q'(T_n) = (\langle m \rangle - 1) + c_\gamma \Delta T_n \ln |\Delta T_n| + O(\Delta T_n),$$

$$H(T_n) = (\langle m \rangle - 1) + d_\gamma \Delta T_n \ln |\Delta T_n| + O(\Delta T_n),$$

where c_γ and d_γ are constants (see Table IV for their expression in the case of a pure power-law distribution q_m). Using these expressions in the definition of λ_n given by Eq. (54) we derive the critical scaling of ψ_n given by

$$\psi_n = 1 - \hat{A}_\gamma \Delta T_n \ln |\Delta T_n| + O(\Delta T_n), \tag{71}$$

where A_γ is given by Eq. (67).
By performing the limit of ψ_n for $n \to \infty$ and using the scaling relation determined in Eq. (27) we obtain

$$\psi = 1 - \tilde{A}_\gamma \Delta p [\ln |\Delta p|]^2 + o[(\Delta p)(\ln |\Delta p|)^2]. \tag{72}$$

(5) Case $2 < \gamma < 3$

Finally in this case the asymptotic expansion of $Q'(T_n)$ and $H(T_n)$ for $\Delta p < 0$ and $\Delta T_n < 0$, $|\Delta T_n| \ll 1$ and $|\Delta p| \ll 1$, is given by

$$Q'(T_n) = (\langle m \rangle - 1) + c_\gamma |\Delta T_n|^{\gamma-2} + o(|\Delta T_n|^{\gamma-2}),$$

$$H(T_n) = (\langle m \rangle - 1) + d_\gamma |\Delta T_n|^{\gamma-2} + o(|\Delta T_n|^{\gamma-2}),$$

where c_γ and d_γ are constants (see Table IV for their expression in the case of a pure power-law distribution q_m). These expressions leads to the critical scaling of ψ_n given by

$$\psi_n = 1 - \hat{A}_\gamma |\Delta T_n|^{\gamma-2} + o(|\Delta T_n|^{\gamma-2}), \tag{73}$$

where A_γ is given by Eq. (67). By performing the limit of ψ_n for $n \to \infty$ and using the scaling relation determined in Eq. (29) with $\beta = 1/(\gamma - 2)$, we obtain the critical behavior of the fractal exponent ψ:

$$\psi = 1 - \tilde{A}_\gamma |\Delta p| + o(|\Delta p|), \tag{74}$$

where $\tilde{A}_\gamma = \hat{A}_\gamma A_\gamma^{\gamma-2}$.

Thus, for a distribution q_m that scales asymptotically as a power law, we find an anomalous exponent ψ that depends upon the scaling exponent γ as described in Table III.

VII. FRACTION OF NODES IN THE GIANT COMPONENT P_∞

A. General framework

In this section our goal is to investigate the nature of the percolation phase transition at the upper critical threshold p_c using RG arguments already introduced in Ref. [48]. For this transition the order parameter is given by the fraction P_∞ of nodes in the giant component in an infinite network,

$$P_\infty = \lim_{n \to \infty} \frac{R_n}{\bar{N}_n}. \tag{75}$$

By using Eq. (45) for approximating R_n when $n \gg 1$ we obtain

$$P_\infty \simeq \lim_{n \to \infty} \frac{1}{\bar{N}_n^{(0)}} \prod_{n'=1}^{n} \lambda_{n'}$$

$$\simeq \exp\left[-\ln[\langle m \rangle - 1] \int_0^\infty dn (1 - \psi_n) \right], \tag{76}$$

where the last expression is derived by using a continuous approximation for n. Therefore in order to evaluate the critical behavior P_∞ we need to know the dependence of ψ_n on n. Close to the percolation threshold, for $0 < p_c - p \ll 1$ we can use Eq. (57) and its explicit expression derived in Sec. VI C in order to express ψ_n as a function of ΔT_n. Finally the dependence of ΔT_n on n can be derived by expanding the RG Eq. (7) close to the upper percolation threshold p_c. In the following we will derive the critical behavior of the order parameter P_∞ by following the inverse order. First, we will derive the functional behavior of ΔT_n on n, then we will use the scaling of ψ_n as a function of ΔT_n to predict the nature of the percolation transition at $p = p_c$ in the continuous approximation. We will consider first the cases in which the second moment $\langle m^2 \rangle$ is convergent, finding that the percolation transition is always discontinuous. Subsequently we will investigate the cases for which q_m has an asymptotic power-law decay $q_m \simeq C m^{-\gamma}$ for $m \gg 1$. In this case we observe as a function of γ different universality classes summarized in Table V. As long as both $\langle m \rangle$ and $\langle m^2 \rangle$ are convergent we always find

TABLE V. Critical behavior of the fraction of nodes $P_\infty(p)$ in the giant component for $p = p_c + \Delta p$ with $0 < \Delta p \ll 1$, and the nature of the phase transition (continuous or discontinuous) for random hyperbolic manifolds with q_m having power-law asymptotic scaling $q_m \simeq C m^{-\gamma}$, for $m \gg 1$.

γ	Expansion of $P_\infty(p_c + \Delta p)$	Nature of transition
$\gamma > 4$	$P_\infty(p_c) - \alpha_\gamma \Delta p \ln \Delta p$	Discontinuous
$\gamma = 4$	$P_\infty(p_c) + \alpha_\gamma \Delta p [\ln \Delta p]^2$	Discontinuous
$\gamma \in (3, 4)$	$P_\infty(p_c) + \alpha_\gamma \Delta p^{\gamma-3}$	Discontinuous
$\gamma = 3$	$\alpha_\gamma e^{-\delta/\Delta p}$	Continuous
$\gamma \in (2, 3)$	$\alpha_\gamma \Delta p^{\hat{\beta}}$	Continuous

discontinuous transitions, although the universality classes as a function of γ varies determining different critical scalings. When $\langle m^2 \rangle$ is divergent we find instead that the percolation transition becomes continuous. Our approach uses the continuous approximation, and to validate this approach our analytical results are compared with exact numerical results performed for very large number of iterations n in the case of deterministic hyperbolic manifolds. The case of a power-law distribution q_m is, however, studied only analytically due to the very slow convergence of the numerical calculations, in particular close to the critical point.

B. Case of arbitrary q_m distribution with convergent second moment $\langle m^2 \rangle$

1. RG flow

Here we consider arbitrary q_m distributions with convergent second moment $\langle m^2 \rangle$, and we derive in the continuous approximation the dependence of ΔT_n on n. Our starting point is the RG Eq. (7) that we rewrite here for convenience

$$T_{n+1} = F(p, T_n) = p + (1-p) \sum_m q_m T_n^{m-1}. \quad (77)$$

By developing this equation close to the critical point $(p, T) = (p_c, T_c)$ and indicating with $\Delta p = p - p_c > 0$ and $\Delta T_n = T - T_c$ we get

$$T_{n+1} = F(p_c, T_c) + \frac{\partial F}{\partial p}\bigg|_{p=p_c, T=T_c} \Delta p$$
$$+ \frac{\partial F}{\partial T}\bigg|_{p=p_c, T=T_c} \Delta T_n + \frac{\partial^2 F}{\partial p \partial T}\bigg|_{p=p_c, T=T_c} \Delta p \Delta T_n$$
$$+ \frac{1}{2} \frac{\partial^2 F}{\partial T^2}\bigg|_{p=p_c, T=T_c} (\Delta T_n)^2 + \cdots, \quad (78)$$

with

$$F(p_c, T_c) = T_c = 1, \quad (79)$$

$$\frac{\partial F}{\partial p}\bigg|_{p=p_c, T=T_c} = 0, \quad (80)$$

$$\frac{\partial F}{\partial T}\bigg|_{p=p_c, T=T_c} = 1, \quad (81)$$

$$\frac{\partial^2 F}{\partial p \partial T}\bigg|_{p=p_c, T=T_c} = -\langle m-1 \rangle, \quad (82)$$

$$\frac{\partial^2 F}{\partial T^2}\bigg|_{p=p_c, T=T_c} = \frac{\langle (m-1)(m-2) \rangle}{\langle m-1 \rangle}. \quad (83)$$

Therefore by truncating the expansion to the leading terms in ΔT_n and Δp we can write

$$\Delta T_{n+1} - \Delta T_n = \hat{C} \Delta T_n [\Delta T_n - \hat{B} \Delta p], \quad (84)$$

with the constants $\hat{B}$ and $\hat{C}$ given by

$$\hat{B} = \frac{2\langle m-1 \rangle^2}{\langle (m-1)(m-2) \rangle}, \quad (85)$$

$$\hat{C} = \frac{1}{2} \frac{\langle (m-1)(m-2) \rangle}{\langle m-1 \rangle}. \quad (86)$$

For $n \to \infty$ we approximate Eq. (84) in the continuous limit, and we use x to indicate the continuous approximation of $-\Delta T_n \ll 1$, i.e., $x \simeq -\Delta T_n$. In this way we get the differential equation

$$\frac{dx}{dn} = -\hat{C} x[x + \hat{B} \Delta p], \quad (87)$$

with initial condition $x(0) = 1 - p$, whose solution is

$$x(n) = \hat{B} \Delta p \left[\left(1 + \frac{\hat{B} \Delta p}{1-p} \right) e^{\hat{C} \hat{B} (\Delta p) n} - 1 \right]^{-1}. \quad (88)$$

2. Case in which both $\langle m^2 \rangle$ and $\langle m^3 \rangle$ are convergent

This case includes all distributions q_m which have a convergent first, second, and third moment $\langle m \rangle$, $\langle m^2 \rangle$, and $\langle m^3 \rangle$. Consequently it includes the deterministic hyperbolic manifold with $q_{m'} = \delta_{m,m'}$ and the random hyperbolic manifold with asymptotic power-law scaling of $q_m \simeq C m^{-\gamma}$ with $\gamma > 4$. For this case ψ_n obeys the scaling relation Eq. (58), which we rewrite here for convenience:

$$\psi_n = 1 - \hat{A}(T_c - T_n)^2 = 1 - \hat{A}[x(n)]^2. \quad (89)$$

Therefore using Eq. (76) we can express P_∞ in the continuous approximation as

$$P_\infty(p) \simeq \exp\left[-\ln\langle m-1 \rangle \hat{A} \int dn [x(n)]^2 \right]. \quad (90)$$

By inserting the expression of $x(n)$ derived in Eq. (88) we obtain for $0 < p - p_c \ll 1$

$$P_\infty(p) \simeq \exp\left\{ -\ln(\langle m \rangle - 1)\hat{A}_m \right.$$
$$\left. \times \left[\frac{(1-p)}{\hat{C}} + \frac{\hat{B} \Delta p}{\hat{C}} \ln\left(\frac{\hat{B} \Delta p}{\hat{C}} \right) \right] \right\}, \quad (91)$$

which can be also written as

$$P_\infty(p) \simeq P_\infty(p_c) \left(\frac{\Delta p}{r} \right)^{-h \Delta p}, \quad (92)$$

where $P_\infty(p_c)$, h, and r are given by

$$P_\infty(p_c) = \exp\left[-\ln(\langle m \rangle - 1)\hat{A} \frac{2}{\langle (m-1)(m-2) \rangle} \right],$$
$$h = \ln(\langle m \rangle - 1)\hat{A} \frac{\hat{B}}{\hat{C}},$$
$$r = \frac{\hat{C}}{\hat{B} \langle m-1 \rangle}. \quad (93)$$

Equation (92) can be further expanded for $0 < \Delta p \ll 1$, obtaining the critical behavior

$$P_\infty(p) \simeq P_\infty(p_c) + \alpha \Delta p [-\ln(\Delta p)], \quad (94)$$

where $\alpha = P_\infty(p_c) h$. This expression clearly shows that in this case the transition is discontinuous and the fraction of nodes in the giant component has a discontinuity of $P_\infty(p_c) > 0$ at the critical point. However, this is not an ordinary first-order transition as dP_∞/dp diverges logarithmically as $\ln(\Delta p)$.

The deterministic hyperbolic manifolds having $q_{m'} = \delta_{m',m}$ deserves some special attention. In this case we have that $\hat{A}$ is
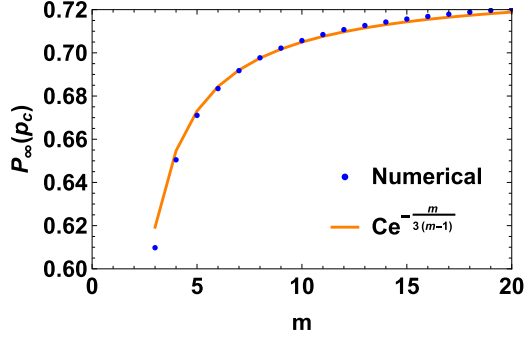
FIG. 8. The discontinuity $P_\infty(p_c)$ of the order parameter P_{inf} at the critical point $p = p_c$ is numerically evaluated for deterministic hyperbolic manifolds with $3 \leqslant m \leqslant 20$ evolved up to $n = 1000$ iterations. These numerical results agree well with the analytical expression in Eq. (95) up to a multiplicative constant $C = 1.021 \ldots$.

expressed by Eq. (59), which we rewrite here for convenience:

$$\hat{A} = \hat{A}_m = \frac{1}{6} \frac{m(m-2)}{\ln(m-1)},$$

and the size of the discontinuity $P_\infty(p_c)$ in the size of the giant component at the upper percolation threshold is given by

$$P_\infty(p_c) \simeq \exp\left[-\frac{1}{3} \frac{m}{(m-1)}\right]. \tag{95}$$

Moreover the constants h and r take the simple form

$$h = \frac{2}{3} \frac{m(m-1)}{(m-2)}, \tag{96}$$

$$r = \left[\frac{m-2}{2(m-1)}\right]^2. \tag{97}$$

These predictions can be validated by exact numerical integrations of the equations, which provides the fraction P_∞ of nodes in the giant component when the manifold includes n iterations of its recursive construction. In Fig. 8 we show the numerical results obtained for the discontinuity $P_\infty(p_c)$ at the critical point $p = p_c$ for different values of m obtained after $n = 1000$ iterations, and we compare these results with the expression provided in Eq. (95) obtained by neglecting the nonhomogeneous terms in Eq. (41) and performing the continuous approximation for solving the RG flow equations. The analytical expression differs from the exact numerical results only by a multiplicative constant $C = 1.021 \ldots$. In Fig. 9 we validate Eq. (92) characterizing the scaling of the order parameter $P_\infty(p)$ for $0 < \Delta p = p - p_c \ll 1$ in the case of the deterministic manifolds with $m = 3, 4$. The predicted scaling is confirmed, and the expression of the constant h given by Eq. (96) is a valid approximation; however, for $m = 3$ the value of the constant r deviates from the predicted value given by Eq. (97).

3. Case in which $\gamma = 4$

When the distribution q_m has a power-law asymptotic scaling for $m \gg 1$ given by $q_m \simeq Cm^{-\gamma}$ and $\gamma = 4$ we have shown in Sec. VI C that ψ_n obeys the scaling

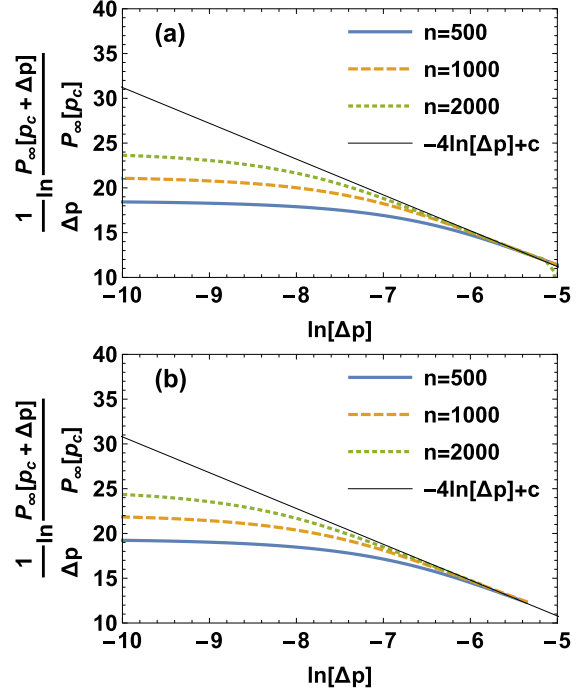$$\psi_n \simeq 1 - \hat{A}_\gamma (\Delta T_n)^2 \ln|\Delta T_n|. \tag{98}$$

FIG. 9. The critical scaling of $P_\infty(p)$ for $0 < \Delta p = p - p_c \ll 1$ is numerically investigated for deterministic hyperbolic manifolds with $m = 3$ (a) and $m = 4$ (b). By investigating the finite-size effects by considering a number of iterations $n = 500, 1000, 2000$ we validate our analytical expression Eq. (92). The constant indicates $c = 4 \ln 9$ for both panels (a) and (b).

Therefore using the continuous approximation expression for $P_\infty(p)$ given by Eq. (76) we obtain

$$P_\infty(p) \simeq \exp\left\{-\ln(\langle m \rangle - 1)\hat{A}_\gamma \int_0^\infty dn[x(n)]^2 \ln[x(n)]\right\}.$$

By inserting the expression of $x(n)$ given by Eq. (88) in the integral appearing in this exponent we obtain

$$\int_0^\infty dn[x(n)]^2 \ln[x(n)]$$

$$= \frac{\hat{B}\Delta p}{\hat{C}} \int_{(1+\frac{\hat{B}\Delta p}{1-p})}^\infty dw \frac{1}{w}(w-1)^{-2} \ln[\hat{B}\Delta p(w-1)^{-1}]$$

$$= \left[(1-p)\ln\left(\frac{1-p}{e}\right) + \frac{1}{2}\hat{B}\Delta p(\ln \hat{B}\Delta p)^2\right]. \tag{99}$$

Therefore for $0 < \Delta p \ll 1$ we obtain the critical behavior

$$P_\infty(p) \simeq P_\infty(p_c) + \alpha_\gamma \Delta p(\ln \Delta p)^2, \tag{100}$$

where $P_\infty(p_c)$ and α_γ are given by

$$P_\infty(p_c) = \left[(\langle m \rangle - 1)\frac{1-p}{e}\right]^{-(1-p)\hat{A}_\gamma},$$

$$\alpha_\gamma = -\frac{\ln(\langle m \rangle - 1)}{2} P_\infty(p_c)\hat{A}_\gamma \hat{B}. \tag{101}$$

Therefore in this case dP_∞/dp diverges as $(\ln \Delta p)^2$.

4. Case in which $\gamma \in (3, 4)$

When the distribution q_m has power-law asymptotic scaling $q_m \simeq C m^{-\gamma}$ for $m \gg 1$ and $\gamma \in (3, 4)$ we have shown in Sec. VI C that ψ_n scales like

$$\psi_n = 1 - \hat{A}_\gamma |\Delta T_n|^{\gamma-2} = 1 - \hat{A}_\gamma [x(n)]^{\gamma-2}. \quad (102)$$

Therefore the fraction $P_\infty(p)$ of nodes in the giant component can be evaluated in the continuous approximation as

$$P_\infty(p) \simeq \exp\left\{-\ln(\langle m \rangle - 1)\hat{A}_\gamma \int_0^\infty dn [x(n)]^{\gamma-2}\right\}.$$

The integral in the exponent of this expression can be performed by using the explicit expression of $x(n)$ given by Eq. (88) obtaining

$$\int_0^\infty dn [x(n)]^{\gamma-2}$$

$$= \int_0^\infty dn (\hat{B}\Delta p)^{\gamma-2} \left[\left(1 + \frac{B\Delta p}{1-p}\right) e^{\hat{B}\hat{C}\Delta pn} - 1\right]^{-(\gamma-2)}$$

$$= \frac{(\hat{B}\Delta p)^{\gamma-3}}{\hat{C}} \int_{(1+\frac{B\Delta p}{1-p})}^\infty dw \frac{1}{w}[w-1]^{-(\gamma-2)}$$

$$\simeq \frac{(1-p)^{\gamma-3}}{\hat{C}(\gamma-3)} - D_\gamma(\Delta p)^{\gamma-3}, \quad (103)$$

where D_γ is a constant. Therefore for $0 < \Delta p \ll 1$ we obtain the critical behavior

$$P_\infty(p) \simeq P_\infty(p_c) + \alpha_\gamma(\Delta p)^{\gamma-3} \quad (104)$$

characteristic of *hybrid phase transitions* where $P_\infty(p_c)$ and α_γ are given by

$$P_\infty(p_c) = \exp\left[-\ln(\langle m \rangle - 1)\hat{A}_\gamma \frac{(1-p)^{\gamma-3}}{\hat{C}(\gamma-3)}\right],$$

$$\alpha_\gamma = P_\infty(p_c)\ln(\langle m \rangle - 1)\hat{A}_\gamma D_\gamma. \quad (105)$$

Therefore in this case a discontinuous phase transition is expected. However, dP_∞/dp diverges as $(\Delta p)^{\gamma-4}$.

C. Convergent $\langle m \rangle$, divergent $\langle m^2 \rangle$

1. Case in which $\gamma = 3$

Here we consider random hyperbolic manifolds with a q_m distribution having an asymptotic power-law scaling $q_m \simeq C m^{-\gamma}$ for $m \gg 1$ with $\gamma = 3$. In this case, by expanding the RG Eq. (7) close to the upper percolation threshold for small ΔT_n and Δp we obtain

$$\Delta T_{n+1} - \Delta T_n = \Delta T_n[-\langle m - 1 \rangle \Delta p + d_\gamma(\Delta T_n)\ln|\Delta T_n|],$$

where we have truncated the expansion by taking only the leading terms in Δp and ΔT_n. In the continuous approximation we get the differential equation

$$\frac{dx}{dn} = -\bar{C}x[x \ln x + \bar{B}\Delta p], \quad (106)$$

with initial condition $x(0) = 1 - p$. This differential equation does not have an explicit analytical solution. In order to find an approximate solution we consider two different ranges of values of n. The first range of values of n is $n < n^\star$

where $n^\star$ satisfies $x(n^\star)\ln x(n^\star) = B\Delta p$. In this regime we observe $x(n)\ln x(n) > B\Delta p$. The second range is $n > n^\star$ where we observe $x(n)\ln x(n) < B\Delta p$. Therefore we can integrate Eq. (106) from $x(0)$ to $x(n^\star)$ and consider the first term of the expansion for $x(n)\ln x(n)/(B\Delta p) \ll 1$. Subsequently we can integrate Eq. (106) from $x(n^\star)$ to a generic $x(n) < x(n^\star)$ and consider only the first term of the expansion for $B\Delta p/[x(n)\ln x(n)] \ll 1$. We note that $n^\star$ is determined by

$$x(n^\star) = \frac{B\Delta p}{\ln[B\Delta p]}. \quad (107)$$

For $n < n^\star$ we obtain that the leading term of the solution of Eq. (106) reads

$$\text{Ei}[\ln(x(n))] - \text{Ei}[\ln(1-p)] = -\bar{C}n, \quad (108)$$

where $\text{Ei}(z)$ indicates the exponential integral function. We note that as expected this solution obtained by considering the leading term in $x(n)\ln(x)/[B\Delta p]$ is independent of Δp as expected. For $n > n^\star$ we obtain instead

$$x(n) = x(n^\star)e^{-\bar{B}\bar{C}\Delta p(n-n^\star)}. \quad (109)$$

As we have shown in Sec. VI C the asymptotic scaling of ψ_n for $\gamma = 3$ is given by

$$\psi_n \simeq 1 - \hat{A}_\gamma x(n)\ln x(n). \quad (110)$$

Therefore, by inserting this scaling in Eq. (76) we get

$$P_\infty \simeq \exp\left\{-\ln(\langle m \rangle - 1)\hat{A}_\gamma \int_0^\infty dn x(n)\ln x(n)\right\}$$

$$\times \exp\left\{\phi - \ln(\langle m \rangle - 1)\hat{A}_\gamma \int_{n^\star}^\infty dn x(n)\ln x(n)\right\},$$

where in the second expression the constant ϕ is given by

$$\phi = \int_0^{n^\star} dn x(n)\ln x(n). \quad (111)$$

By using Eq. (113) to express $x(n)$ for $n > n^\star$ in the equation for $P_\infty(p)$ we can determine the critical scaling of $P_\infty(p)$ close to the upper percolation threshold, given by

$$P_\infty(p) \simeq \alpha_\gamma e^{-\delta/\Delta p}, \quad (112)$$

where $\delta = x(n^\star)/(\bar{B}\bar{C})$ and $\alpha_\gamma = e^\phi$. Therefore in this case the transition is continuous and displays a critical behavior with an effective *"infinite dynamical exponent,"* which has been observed also for percolation in random scale-free networks [25].

2. Case $\gamma \in (2, 3)$

Here we consider random hyperbolic manifolds with a q_m distribution having an asymptotic power-law scaling $q_m \simeq C m^{-\gamma}$ for $m \gg 1$ with $\gamma \in (2, 3)$. In this case, proceeding as in the previous cases and expanding the RG Eq. (7) close to the upper percolation threshold for small ΔT_n and Δp we obtain

$$\Delta T_{n+1} - \Delta T_n = \Delta T_n[-\langle m - 1 \rangle \Delta p + d_\gamma(\Delta T_n)^{\gamma-2}].$$

In the continuous approximation we get the differential equation

$$\frac{dx}{dn} = -d_\gamma x[x^{\gamma-2} + \tilde{B}\Delta p], \quad (113)$$

with initial condition $x(0) = 1 - p$ and with $\tilde{B}$ given by

$$\tilde{B} = \frac{\langle m \rangle - 1}{d_\gamma}. \qquad (114)$$

Equation (109) has the solution

$$x(n) = \left\{ \left[(1-p)^{2-\gamma} + \frac{1}{\tilde{B}\Delta p} \right] e^{d_\gamma \tilde{B}(\Delta p)n} - \frac{1}{\tilde{B}\Delta p} \right\}^{-1/(\gamma-2)}.$$

Since, as we have shown in Sec. VIC for this range of γ values, ψ_n obeys the scaling

$$\psi_n \simeq 1 - \hat{A}_\gamma [x(n)]^{\gamma-2}, \qquad (115)$$

by using Eq. (76) we can express the fraction P_∞ of nodes in the giant component as

$$\ln P_\infty(p) = \exp \left\{ -\hat{A}_\gamma \ln(\langle m \rangle - 1) \int_0^\infty dn [x(n)]^{\gamma-2} \right\}.$$

Finally by inserting the expression for $x(n)$ given by Eq. (115) we get for $0 < \Delta p \ll 1$

$$\int_0^\infty dn [x(n)]^{\gamma-2}$$
$$= \int_0^\infty dn \left\{ \left[(1-p)^{2-\gamma} + \frac{1}{\tilde{B}\Delta p} \right] e^{d_\gamma \tilde{B}(\Delta p)n} - \frac{1}{\tilde{B}\Delta p} \right\}^{-1}$$
$$= -\frac{\ln[\hat{B}\Delta p(1-p)^{2-\gamma}]}{d_\gamma [1 + \tilde{B}\Delta p(1-p)^{2-\gamma}]}$$
$$\simeq -\frac{1}{d_\gamma} \ln \Delta p + D_\gamma, \qquad (116)$$

where D_γ is a constant. Therefore the transition is continuous with the critical behavior

$$P_\infty(p) \simeq \alpha_\gamma (\Delta p)^{\hat{\beta}}, \qquad (117)$$

with $\alpha_\gamma = \exp[-\hat{A}_\gamma \ln(\langle m \rangle - 1)D_\gamma]$ and the dynamical exponent $\hat{\beta}$ given by

$$\hat{\beta} = \frac{\hat{A}_\gamma \ln\langle m - 1 \rangle}{d_\gamma}. \qquad (118)$$

VIII. CONCLUSIONS

In conclusion, we have presented a comprehensive renormalization group study of link percolation in two-dimensional hyperbolic manifolds. The considered manifolds are the skeletons of two-dimensional cell complexes and are iteratively constructed by gluing polygons to links. In particular we have considered the deterministic hyperbolic manifolds formed by identical polygons of size m and random hyperbolic manifolds constructed by gluing polygons of size m drawn from a distribution q_m. Link percolation on deterministic hyperbolic manifolds with $m = 3$ (Farey graphs) has been previously shown [16] to display a discontinuous phase transition at the upper percolation threshold. Here we extend these results by predicting that for any fixed value of m the transition remains discontinuous, and we analytically estimate the discontinuity, finding very good agreement with exact numerical results. For deterministic hyperbolic manifolds, the critical behavior deviates from the one expected for a first-order phase transition as the derivative of the order parameter diverges logarithmically close to the upper percolation threshold p_c. The study of random hyperbolic manifolds with power-law distribution q_m shows a rich set of different universality classes depending on the value of γ. In particular for $\gamma \in (3, 4)$ we predict a hybrid phase transition, while for $\gamma \in (2, 3]$ the transition is predicted to be continuous. Therefore this work reveals that in hyperbolic manifolds a power-law q_m distribution can have a profound effect on the universality class of the link percolation transition at the upper percolation threshold. In this work this phenomena is compared with the well-known effect that power-law degree distributions have on the percolation properties of random networks. This comparison allows us to propose a mathematical mapping between the equation for the percolation probability and the equation determining the probability that by following a link we reach a node in the giant component of a random network. However, the equations determining the order parameter in the hyperbolic manifold do not appear to have an equivalent counterpart in the percolation of random networks.

We hope that this work will stimulate further research in the interplay between network geometry and dynamics and in particular in the properties of percolation in hyperbolic and nonamenable networks.

[1] G. Bianconi, EPL (Europhys. Lett.) **111**, 56001 (2015).

[2] V. Salnikov, D. Cassese, and R. Lambiotte, Euro. J. Phys. **40**, 014001 (2018).

[3] G. Bianconi and C. Rahmede, Phys. Rev. E **93**, 032315 (2016).

[4] D. Mulder and G. Bianconi, J. Stat. Phys. **173**, 783 (2018).

[5] G. Bianconi and C. Rahmede, Sci. Rep. **7**, 41974 (2017).

[6] W.-M. Song, T. Di Matteo, and T. Aste, Phys. Rev. E **85**, 046115 (2012).

[7] Z. Zhang and F. Comellas, Theor. Comput. Sci. **412**, 865 (2011).

[8] J. S. Andrade Jr., H. J. Herrmann, R. F. S. Andrade, and L. R. Da Silva, Phys. Rev. Lett. **94**, 018702 (2005).

[9] G. Bianconi and R. M. Ziff, Phys. Rev. E **98**, 052308 (2018).

[10] A. P. Millán, J. J. Torres, and G. Bianconi, Sci. Rep. **8**, 9910 (2018).

[11] P. S. Skardal and A. Arenas, Phys. Rev. Lett. **122**, 248301 (2019).

[12] I. Iacopini, G. Petri, A. Barrat, and V. Latora, Nat. Commun. **10**, 2485 (2019).

[13] R. Kleinberg, in *IEEE INFOCOM 2007—26th IEEE International Conference on Computer Communications* (IEEE, New York, 2007), pp. 1902–1909.

[14] M. Boguná, F. Papadopoulos, and D. Krioukov, Nat. Comm. **1**, 62 (2010).

[15] A. Faqeeh, S. Osat, and F. Radicchi, Phys. Rev. Lett. **121**, 098301 (2018).

[16] S. Boettcher, V. Singh, and R. M. Ziff, Nat. Comm. **3**, 787 (2012).

[17] I. Benjamini and O. Schramm, J. Am. Math. Soc. **14**, 487 (2001).

[18] H. Gu and R. M. Ziff, Phys. Rev. E **85**, 051141 (2012).

[19] S. Mertens and C. Moore, Phys. Rev. E **96**, 042116 (2017).

[20] D. M. Auto, A. A. Moreira, H. J. Herrmann, and J. S. Andrade Jr., Phys. Rev. E **78**, 066112 (2008).

[21] D. S. Callaway, M. E. J. Newman, S. H. Strogatz, and D. J. Watts, Phys. Rev. Lett. **85**, 5468 (2000).

[22] R. Cohen, K. Erez, D. ben-Avraham, and S. Havlin, Phys. Rev. Lett. **85**, 4626 (2000).

[23] R. Cohen, D. ben-Avraham, and S. Havlin, Phys. Rev. E **66**, 036113 (2002).

[24] S. N. Dorogovtsev and J. F. Mendes, *Evolution of Networks: From Biological Nets to the Internet and WWW* (Oxford University Press, Oxford, 2013).

[25] S. N. Dorogovtsev, A. V. Goltsev, and J. F. F. Mendes, Rev. Mod. Phys. **80**, 1275 (2008).

[26] N. Araújo, P. Grassberger, B. Kahng, K. Schrenk, and R. Ziff, Euro. Phys. J, Special Topics **223**, 2307 (2014).

[27] D. Lee, B. Kahng, Y. Cho, K.-I. Goh, and D.-S. Lee, J. Korean Phys. Soc. **73**, 152 (2018).

[28] I. Kryven, Phys. Rev. E **95**, 052303 (2017).

[29] I. Kryven, Nat. Commun. **10**, 404 (2019).

[30] G. Bianconi, *Multilayer Networks: Structure and Function* (Oxford University Press, Oxford, 2018).

[31] S. V. Buldyrev, R. Parshani, G. Paul, H. E. Stanley, and S. Havlin, Nature (London) **464**, 1025 (2010).

[32] S.-W. Son, G. Bizhani, C. Christensen, P. Grassberger, and M. Paczuski, EPL (Europhysics Lett.) **97**, 16006 (2012).

[33] G. J. Baxter, S. N. Dorogovtsev, A. V. Goltsev, and J. F. F. Mendes, Phys. Rev. Lett. **109**, 248701 (2012).

[34] D. Achlioptas, R. M. D'Souza, and J. Spencer, Science **323**, 1453 (2009).

[35] R. M. Ziff, Phys. Rev. Lett. **103**, 045701 (2009).

[36] R. A. da Costa, S. N. Dorogovtsev, A. V. Goltsev, and J. F. F. Mendes, Phys. Rev. Lett. **105**, 255701 (2010).

[37] O. Riordan and L. Warnke, Science **333**, 322 (2011).

[38] Y. S. Cho, J. S. Lee, H. J. Herrmann, and B. Kahng, Phys. Rev. Lett. **116**, 025701 (2016).

[39] S. M. Oh, S.-W. Son, and B. Kahng, Phys. Rev. E **98**, 060301(R) (2018).

[40] G. Bianconi, Phys. Rev. E **97**, 022314 (2018).

[41] M. Aizenman and C. M. Newman, Comm. Math. Phys. **107**, 611 (1986).

[42] M. Aizenman, J. Chayes, L. Chayes, and C. Newman, J. Stat. Phys. **50**, 1 (1988).

[43] S. Boettcher, J. L. Cook, and R. M. Ziff, Phys. Rev. E **80**, 041115 (2009).

[44] V. Singh and S. Boettcher, Phys. Rev. E **90**, 012117 (2014).

[45] R. M. Ziff, private communication (2018).

[46] T. Nogawa and T. Hasegawa, Phys. Rev. E **89**, 042803 (2014).

[47] T. Hasegawa, M. Sato, and K. Nemoto, Phys. Rev. E **82**, 046101 (2010).

[48] T. Nogawa, J. Phys. A **51**, 505003 (2018).

[49] S. Boettcher and C. Brunson, EPL (Europhysics Lett.) **110**, 26005 (2015).

[50] M. Hinczewski and A. N. Berker, Phys. Rev. E **73**, 066126 (2006).

[51] S. Boettcher and C. T. Brunson, Phys. Rev. E **83**, 021103 (2011).

[52] V. Singh, C. T. Brunson, and S. Boettcher, Phys. Rev. E **90**, 052119 (2014).